

Imène Hermassi<sup>1</sup> / Sofien Azzouz<sup>1</sup> / Lamine Hassini<sup>1</sup> / Ali Belghith<sup>1</sup>

# Moisture Diffusivity of Seedless Grape undergoing convective drying

<sup>1</sup> Laboratoire d'Energétique et des Transferts Thermique et Massique (LETTM), Département de Physique, Faculté des Sciences de Tunis, Université de Tunis El Manar, Tunis, Tunisia, E-mail: imenhermassi@yahoo.fr. <http://orcid.org/0000-0003-4938-9267>.

## Abstract:

Seedless grape (*Sultana grape*) is a very important commercial fruit grown in large quantities in Tunisia. This product is characterized by a high initial moisture content (the initial wet basis moisture content of the fruit is more than 80 %), and thus a high shrinkage during drying. The mature seedless grape is a spherically shaped fruit. Thermo-physical properties and drying kinetics of seedless grape is essential for the optimization of its drying processes. This paper is composed of two parts, the first one is reserved to the experimental study of seedless grapes, such as the establishment of the desorption isotherms which were determined at 40, 50, 60 and 70 °C by using static gravimetric method and these desorption data were fitted by GAB model. Then we were interested in measurement of the axial hydrous shrinkage of a grape berry and it was expressed as a function of moisture content. Indeed, the drying kinetics under different controlled conditions of air temperature and relative humidity were realized. In the second part, the moisture diffusivity of the seedless grape was determined by minimizing the sum of square of deviations between the predicted and experimental values of moisture content of convective drying kinetics. The adopted approach was based on a numerical solving of the conservation equation of the solid phase and the equation of diffusion/convection of liquid phase for spherical geometry, coupled by the solid phase velocity due to shrinkage. The moisture diffusivity of seedless grape increased with temperature and was correlated by an Arrhenius-type equation. Indeed, the effect of moisture diffusivity was expressed by an exponential function. The moisture diffusivity of seedless grape ranged between  $3.5610^{-10}$  (m<sup>2</sup>/s) and  $12.610^{-10}$  (m<sup>2</sup>/s). Activation energy was found equal to 57.76 kJ/mol.

**Keywords:** convective drying, seedless grape, desorption isotherms, shrinkage, drying kinetics, moisture diffusivity

**DOI:** 10.1515/cppm-2016-0074

**Received:** November 17, 2016; **Revised:** December 27, 2016; **Accepted:** January 1, 2016

## 1 Introduction

Drying is a complex phenomenon, whose mechanisms are not yet completely understood. During drying of agro-alimentary products, moisture diffusivity presents a very important transport parameter for the calculation of the water transfer inside the product, we can distinguish liquid diffusion, vapor diffusion, surface diffusion and hydrostatic pressure differences [1, 2]. For a good understanding of transfer process during drying for production of quality dried products and in order to conserve energy during seedless grape drying, it is important to know its diffusivity, equilibrium moisture content, shrinkage behavior and drying kinetics [3]. The knowledge of moisture diffusivity coefficient is crucial for simulation and optimization of the drying process. The moisture diffusivity's theory is difficult because the physical properties and composition of products were very complex and different. Shrinkage present one of the undesirable changes which occur simultaneously within moisture diffusivity in drying, it makes changes in physical properties and in the heat and mass exchange surface. In particular, agro-alimentary products have high initial moisture content (dry basis) and endure alterations to their original form during the drying process due to significant shrinkage. Heating and loss of water cause stress in the cellular structure of the food and lead to changes in geometry and decrease in dimensions [4]. All these parameters and deformations influencing in particular the moisture diffusivity coefficient. According to the literature, the evaluation's methods of this coefficient are articulated around two approaches: analytical and numerical. The first one is based on the analytical solution of the second Fickian law and providing a median value of diffusivity [5]. However, the application's conditions of this law are not strictly checked for products with big deformations. The second approach is based on the numerical resolution of drying's models. it with the advantage of taking into account the variation of the shrinkage of the sample

Imène Hermassi is the corresponding author.

©2017 by De Gruyter.

and also the variation of diffusivity according to the moisture content. It should be noted that in our laboratory (LETTM) the moisture diffusivity of the deformable products is determined by a relevant numerical approach. This approach was developed initially by Azzouz et al. [6], improved later by Hassini et al. [7], and it was used with some improvements concerning both the numerical model and the drying experiments used by the model to adjust the moisture diffusivity of seedless grapes [8]. Many research tasks on biological products used the numerical method in order to evaluate the moisture diffusivity coefficient [9, 10].

The aim of this work is to develop a diffusive model which takes into account the shrinkage of the sample. This model is based on experimental drying kinetics to evaluate the moisture diffusivity coefficient of the sultana grape, according to the temperature and the moisture content. The adopted method is based to minimize the difference between average moisture content experimental and calculated by a numerical model of drying.

## 2 Materials and methods

### 2.1 Experimental protocol

#### 2.1.1 Raw material

The experimental study has been performed on samples of fresh seedless grapes (*Sultana grape*) were purchased from a local market (*Tunis, Tunisia*). All the grapes were supplied by the same producer in order to maximize the reproducibility of the results. Moisture content was determined by drying the grape berries 24 h in an oven at 70 °C [11].

#### 2.1.2 Equilibrium moisture content

Desorption isotherms were obtained by keeping the sample at a constant partial pressure of water vapor at a given temperature until reach the hygroscopic equilibrium. This equilibrium was reached when we has not noticed a significant change in the sample weight. Desorption isotherms of seedless grape were determined at several temperatures by a static gravimetric method [12], for placing the sample in a enclosure (Figure 1) by maintaining with fixed temperature and where moisture control is provided by saturated solutions of salts (KOH, MgCl<sub>2</sub>, K<sub>2</sub>CO<sub>3</sub>, NaBr, NaNO<sub>2</sub>, NaCl, KCl and BaCl<sub>2</sub>) which were selected to provide different water activities in the range of 0.1–0.9 (Table 1). The salt solutions and their water activities are taken from literature [13, 14]. The grape berries are suspended in hermetic jars half filled by the various salt solutions, without contact with its solutions. Then the loaded jars were placed in an oven at controlled temperature. The initial mass of the grape berry was about  $3.040 \pm 0.050$  g. Four repetitions were performed (four samples per salt). The glass sorption jars were placed in a vacuum oven at the controlled temperatures of 40, 50, 60 and 70 °C  $\pm 1$  °C. Each sample was carefully weighed every week by using an analytical balance (Mettler, precision:  $10^{-4}$ g) until no significant change in weight was observed between two consecutive measurements [15]. Once equilibrium was reached, the moisture content of the sample was determined by drying 24 h in a vacuum oven at 70 °C [11]. The hygroscopic equilibrium was reached after 2 weeks.

**Table 1:** Saturated salt solutions and corresponding water activities.

Solution	Temperature (°C)			
	40°C	50°C	60°C	70 °C
KOH	0.063	0.057	0.055	0.053
MgCl <sub>2</sub>	0.316	0.304	0.295	0.288
K <sub>2</sub> CO <sub>3</sub>	0.433	0.427	0.421	0.416
NaBr	0.532	0.512	0.491	0.473
NaNO <sub>2</sub>	0.608	0.588	0.565	0.544
NaCl	0.747	0.718	0.703	0.689
KCl	0.823	0.777	0.751	0.727
BaCl <sub>2</sub>	0.891	0.882	0.872	0.863

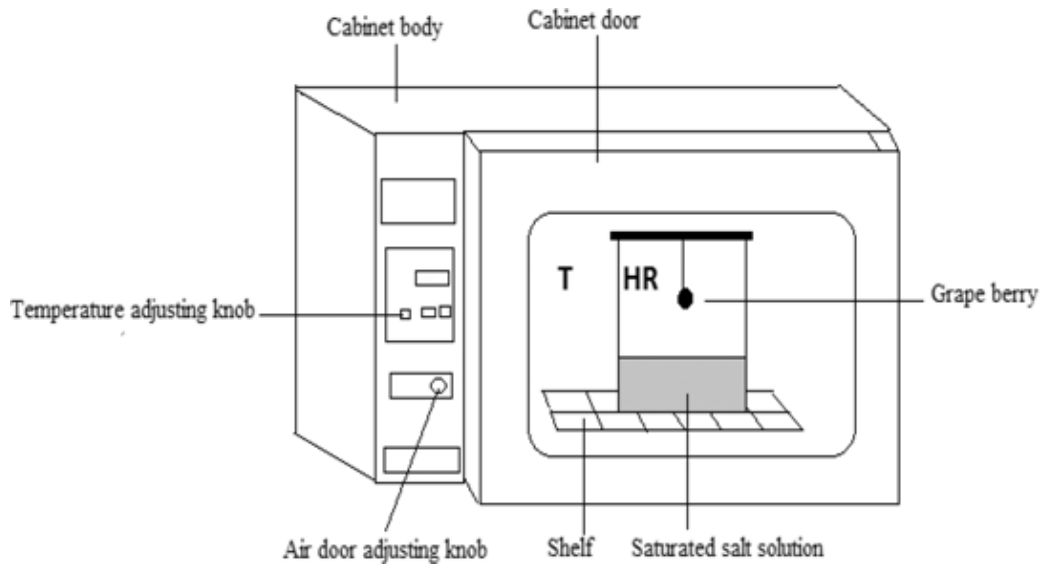


**Figure 1:** Experimental apparatus for determination of desorption isotherms.

Several mathematics models have been developed in literature to describe desorption isotherms for various food products [14]. Our experimental data were best fitted with the Guggenheim, Anderson and de Boer (GAB) model, expressed by the following equation:

$$X_{eq} = \frac{X_m C K a_w}{(1 - K a_w) (1 - K a_w + C K a_w)} \quad (1)$$

The moisture content equilibrium value ( $X_{eq}$ ) was used in the boundary conditions for the moisture diffusivity estimation model.

The adequacy of the model was evaluated by the correlation coefficient ( $r$ ) and the standard error coefficients ( $s$ ) calculated by the software Curve Expert 5.1. These parameters can be calculated as follows:

$$s = \sqrt{\frac{\sum_{i=1}^{n_{exp.data}} (X_{eq} - X_{eq.cali})^2}{n_{exp.data} - n_{param}}} \quad (2)$$

$$r = \sqrt{1 - \frac{\sum_{i=1}^{n_{exp.data}} (X_{eqi} - X_{eq.cali})^2}{\sum_{i=1}^{n_{exp.data}} (\bar{X}_{eq} - X_{eqi})^2}} \quad (3)$$

The arithmetic average value of the experimental equilibrium moisture content ( $\bar{X}_{eq}$ ) was calculated by using this relation [15]:

$$\bar{X}_{eq} = \frac{1}{n_{exp.data}} \sum_{i=1}^{n_{exp.data}} X_{eqi} \quad (4)$$

### 2.1.3 Shrinkage of seedless grape

In drying process some materials behaves like a rigid materials and other contract and undergo shrinkage because the components of a solid structure get tighter influenced by internal forces. The material acts as a saturated porous medium that's no porosity develops and water occupies all of the pores of the solid matrix. Concentration is then characterized by a linear relationship between the shrinkage and the moisture content in a dry basis. The majority of solid matrix still deformable and stops when the matrix reaches a certain threshold of rigidity. The shrinkage of food products occurs simultaneously with the moisture diffusion inside the product and can thus affect the velocity of water loss during drying. Shrinkage experiments were carried out on grapes berries treated of same sizes. These grapes are considered spherical forms. The measurement of the shrinkage consists in following the evolution of the grape size following its two characteristic diameters (horizontal diameter and vertical diameter) at various times of drying [3, 16].

### 2.1.4 Drying kinetics

The experimental drying kinetics were carried out in a climatic blower: convective vertical downward flow with controlled temperature (T), relative humidity (RH) and velocity (u), existing in the laboratory of Energy and Heat and Mass Transfers (LETTM) (Figure 2).

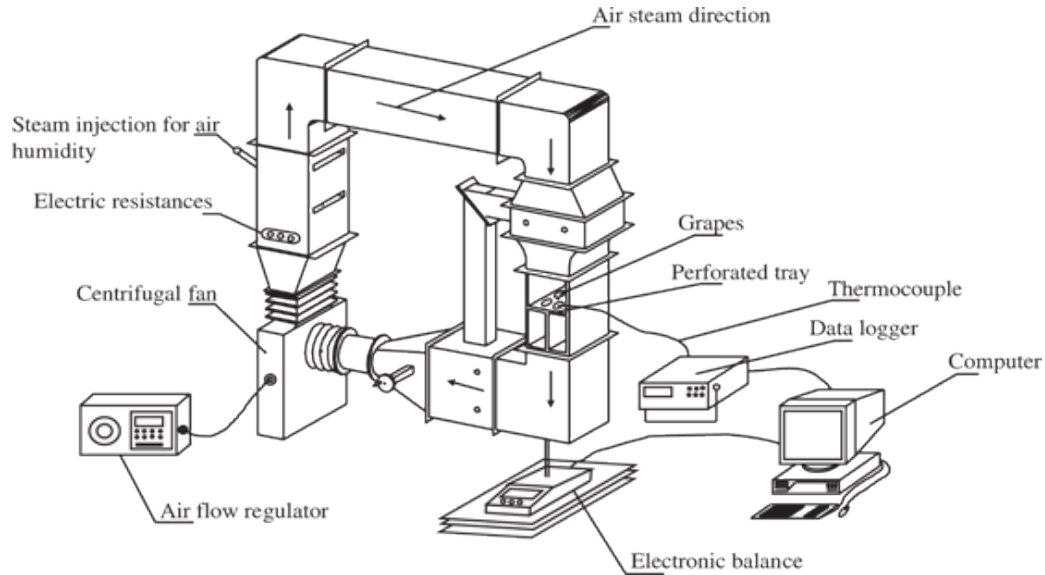


Figure 2: Overall layout of the experimental laboratory dryer.

The grapes berries were placed on a perforated tray which was suspended to an electronic balance with a precision of 0.001 g. The drying experiments were established at four temperatures 40, 50, 60 and 70 °C and regulated to  $\pm 1$  °C and air velocity at 2.5 m/s. The mass of the product was continuously measured with constant time interval (2 min) in each drying temperature and recorded by a microcomputer. The experiments were replicated two times in each temperature in order to check the reproducibility of the drying curves. Drying was stopped when the weight of the test sample remained constant. The dry solid weight of the product was determined after each experiment by the vacuum oven-drying method at 70 °C for 48 h [11].

The dry basis equilibrium moisture content  $X$  (kg water/kg dry matter) is given by the following expression:

$$X = \frac{M_f - M_d}{M_d} \quad (5)$$

## 2.2 Numerical identification of the moisture diffusivity coefficient

The numerical procedure is essential to predict and simulate the drying behavior and it consists on solving the transfer conservation equations of both solid matter and water to take account for the material's shrinkage. The equations are coupled by the solid phase velocity.

In order to facilitate the numerical resolution of the model equations many simplifying assumptions are formulated:

- The transfers of heat and mass are one-dimensional.
- The product is biphasic water-solid.
- Evaporation is carried out on the surface.
- The shrinkage is ideal and isotropic.

The conservation equations of the solid and water phases are written respectively:

$$\frac{\partial c_s}{\partial t} = -\text{div}(c_s u_s) \quad (6)$$

$$\frac{\partial c_l}{\partial t} = -\text{div}(c_l u_l) \quad (7)$$

with:

$$c_s = \frac{\rho_s}{1 + \beta X} \quad (8)$$

$$c_l = c_s X \quad (9)$$

The liquid mass flux is given by Bird et al. [17]:

$$c_l u_l = -\rho D \text{grad} \left( \frac{c_l}{\rho} \right) + c_l u \quad (10)$$

In convective drying of the grape the liquid migrates by diffusion and is transported by the shrinkage.

For an ideal shrinkage model, we can use the followings equations [18]:

$$u = \frac{c_s u_s + c_l u_l}{\rho} \quad (11)$$

$$\rho = c_s + c_l \quad (12)$$

By combining previous equations, we obtain finally the conservation equations of solid and liquid phases in spherical coordinates:

$$\frac{\beta}{1 + \beta X} \frac{\partial X}{\partial t} = \frac{1}{r^2} \frac{\partial}{\partial r} (r^2 u_s) - \frac{u_s \beta}{1 + \beta X} \frac{\partial X}{\partial r} \quad (13)$$

$$\frac{1}{1 + \beta X} \frac{\partial X}{\partial t} = \frac{1}{r^2} \frac{\partial}{\partial r} \left( \frac{r^2 D}{1 + \beta X} \frac{\partial X}{\partial r} \right) - \frac{u_s}{1 + \beta X} \frac{\partial X}{\partial r} \quad (14)$$

Equations 13 and 14 were numerically solved for  $u_s$  and  $X$  using the initial and boundary conditions at the surface ( $r = R$ ) and at the center of a grain ( $r = 0$ ):

$$t = 0; 0 < r < R; X = X_0; u_s = 0 \quad (15)$$

$$t > 0; r = 0; \frac{\partial X}{\partial r} = 0; u_s = 0 \quad (16)$$

$$r = R(t); \left[ \frac{\rho_s}{1 + \beta X} \left( -D \frac{\partial X}{\partial r} + X u_s^r \right) \right] = k_m * \frac{M_v}{R} \left[ \frac{a_w(X, T) * P_{vsat}(T)}{T} - \frac{RH * P_{vsat}(T_a)}{T_a} \right] \quad (17)$$

The saturation vapor pressure was derived from the literature [14]:

$$P_{v,sat} = \exp \left( 52.576 - \frac{6790.5}{(T_a + 273.18)} - 5.281 * \log(T_a + 273.18) \right) \quad (18)$$

The mass transfer coefficient to the level of the grape surface is evaluated starting from the heat transfer coefficient according to the following equation [19]:

$$K_m = \frac{D_a}{d} (2 + 0.552 Re^{0.53} Sc^{0.33}) \quad (19)$$

Reynolds and Schmidt numbers were respectively calculated with the air experimental conditions:

$$Re_L = \frac{\rho v d}{\mu} = \frac{v d}{\nu} \quad (20)$$

$$Sc = \frac{\mu}{\rho D} \quad (21)$$

The control volume spatial discretization with entirely implicit time integration which we were used was developed by Patankar [20]. The total number of calculation nodes over the sample thickness was kept fixed but the control volumes thicknesses were changed at each time step, as the sample thickness changed during drying. The thickness of each control volume was changed independently, according to the local moisture content variation and considering a constant dry solid mass within each control volume [7].

The establishment of moisture diffusivity was carried by the minimization of the difference between the experimental drying kinetics ( $X = f(t)$ ) and the simulated one.

Moisture diffusivity depends on the variation of the moisture content during drying, the physical structure of the products and the experimental drying conditions [21]. Generally the variation of the moisture diffusivity with temperature is represented by Arrhenius equation 8, [22–24]. However the influence of the moisture content has not been performed into a general accepted model. In the present study, the effect of the moisture content is suitable presented by an exponential function [7]:

$$D(X, T) = D_{X1}(T) \exp(D_{X2}(T) X) \quad (22)$$

with:

$$D_{X1}(T) = D_0 \exp\left(-\frac{E_a}{R \cdot T}\right) \quad (23)$$

$$D_{X2}(T) = AT + B \quad (24)$$

### 3 Results and discussion

#### 3.1 Desorption isotherms

The results of the experimental measurement of the desorption isotherms of grapes at 40, 50, 60 and 70 °C are shown in Figure 3. The shape of the isotherms is sigmoid corresponding to type II curves according to BET classification [25], similar to the majority of food products.

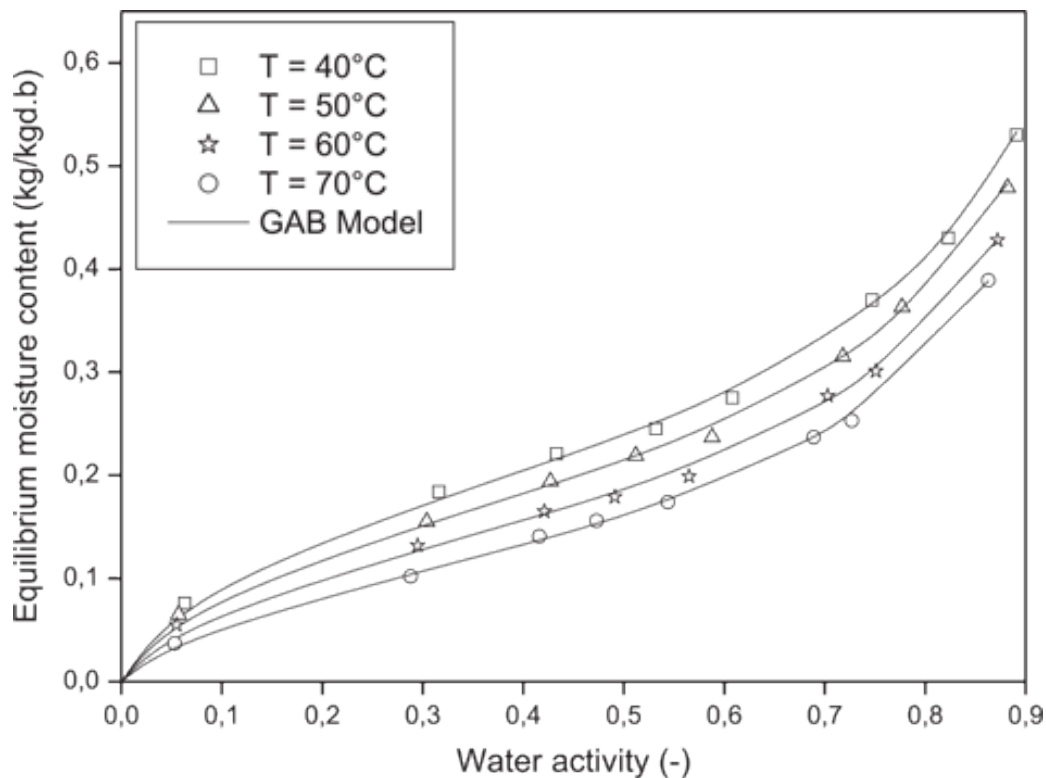


**Figure 3:** Desorption isotherms for prickly seedless grape at various temperatures.

An acceptable agreement between experimental and calculated fit can be observed. Commonly, at each temperature, all experimental data of desorption isotherms, show an increase of the equilibrium moisture data

with increasing of the water activity. In addition, these curves show that the equilibrium moisture content increases when the temperature decreases, which is consistent with the literature [26]. At higher temperature and at a given water activity, the equilibrium moisture content is lower, signifying less hygroscopic capacity due to modifications induced by temperatures in the product and the higher energy levels of the water molecules [27].

The three parameters of the GAB model ( $X_m$ ,  $C$  and  $K$ ) depend on the characteristics of the product and the equilibrium temperature. The values of these parameters at various temperatures and the statistical analysis are given in Table 2.

**Table 2:** Estimated parameters and fitting criteria of the GAB model applied to experimental desorption isotherms data of seedless grape.

Temperature (°C)	$X_m$ (kg/kg d.b)	$C$	$K$	$r$	$S$
40	0.152	18.862	0.803	0.999	0.007
50	0.134	18.128	0.821	0.999	0.004
60	0.113	18.116	0.848	0.999	0.004
70	0.101	11.337	0.865	0.999	0.004

### 3.2 Shrinkage curves

Figure 4 presents the curves of the dimensionless relative diameters characteristics (a) ( $d_v/d_{v0}$ ) and (b) ( $d_h/d_{h0}$ ) of a grape versus the moisture content, for various temperatures of drying. We note that, the shrinkage following vertical diameter  $d_v$  varies linearly lasting all the period of drying. On the other hand, the shrinkage following the horizontal diameter  $d_h$  is constant. This particular evolution of the shrinkage, at the end of drying is explained by the fact why the transfer of water is dominating according to the vertical diameter of the grape. For low moisture content air penetration and development of air-filled porosity in the material at the end of drying.

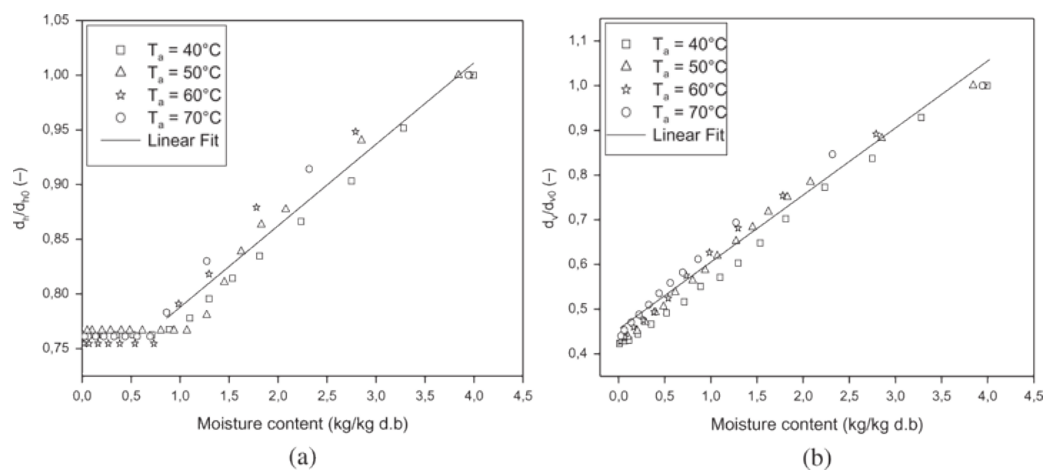


**Figure 4:** Curves of the dimensionless relative diameters characteristics (a) ( $d_v/d_{v0}$ ) and (b) ( $d_h/d_{h0}$ ) of seedless grape.

The predictive correlation of the shrinkage is given by the expressions bellow:

$$\frac{d_v}{d_{v0}} = 0.15X + 0.443; (0.02 \leq X \leq 0.4 \text{ kg/kg d.b}); r = 0.987 \quad (25)$$

$$\frac{d_h}{d_{h0}} = \begin{cases} 0.073X + 0.719; (0.7 \leq X \leq 0.4 \text{ kg/kg d.b}) ; r = 0.978 \\ 0.004X + 0.76; (X \leq 0.7 \text{ kg/kg d.b}) ; r = 0.932 \end{cases} \quad (26)$$

### 3.3 Drying kinetics

The evolution of the drying kinetics as a function of drying time and the variation of the drying rate versus moisture content of Sultana grape at various air conditions, were both shown in Figure 5 and Figure 6. These

curves illustrate the absence of constant drying period, they show only the falling-rate period. This result designate that diffusion is the physical process governing moisture movement in berries grape. We note a reduction in the drying time when the drying air temperature increase. These results are the same for other food products [28].

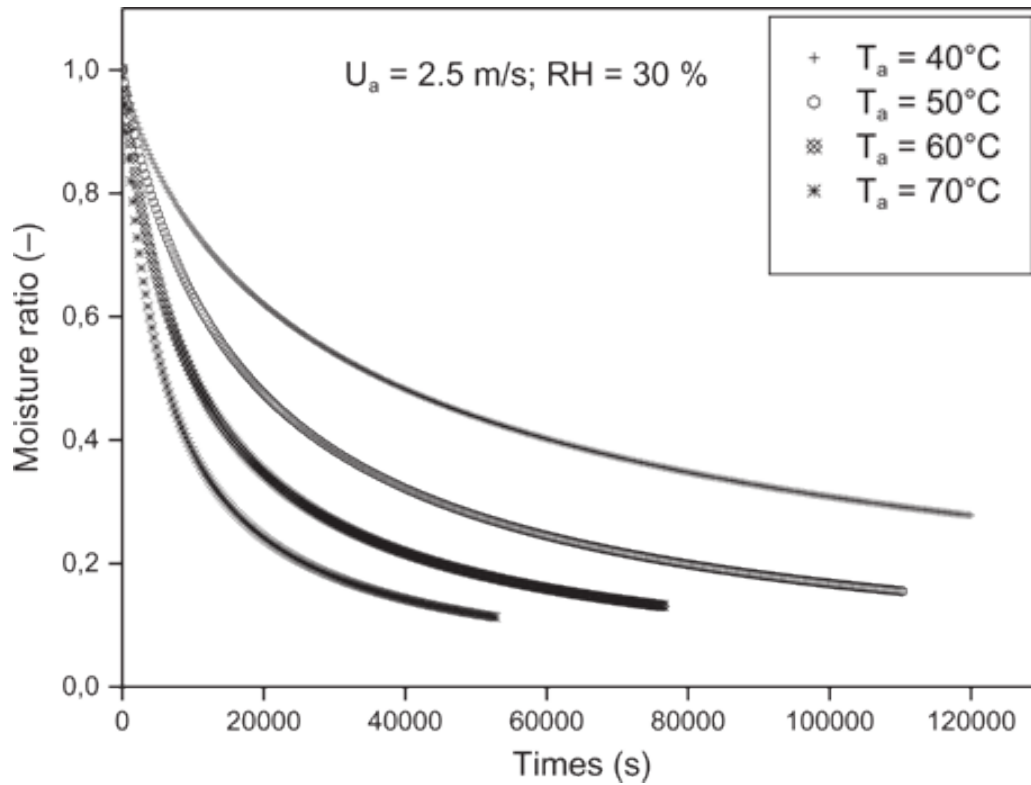


Figure 5: Variation of moisture content of Sultana grape versus drying time at different air temperatures.

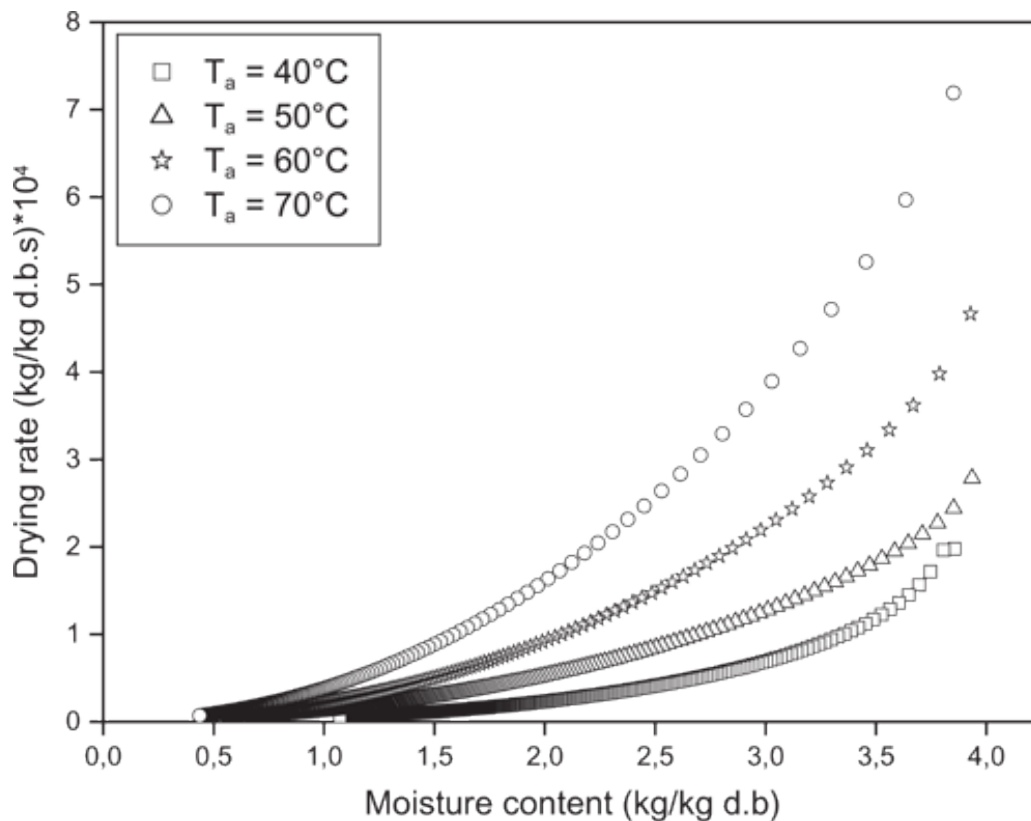
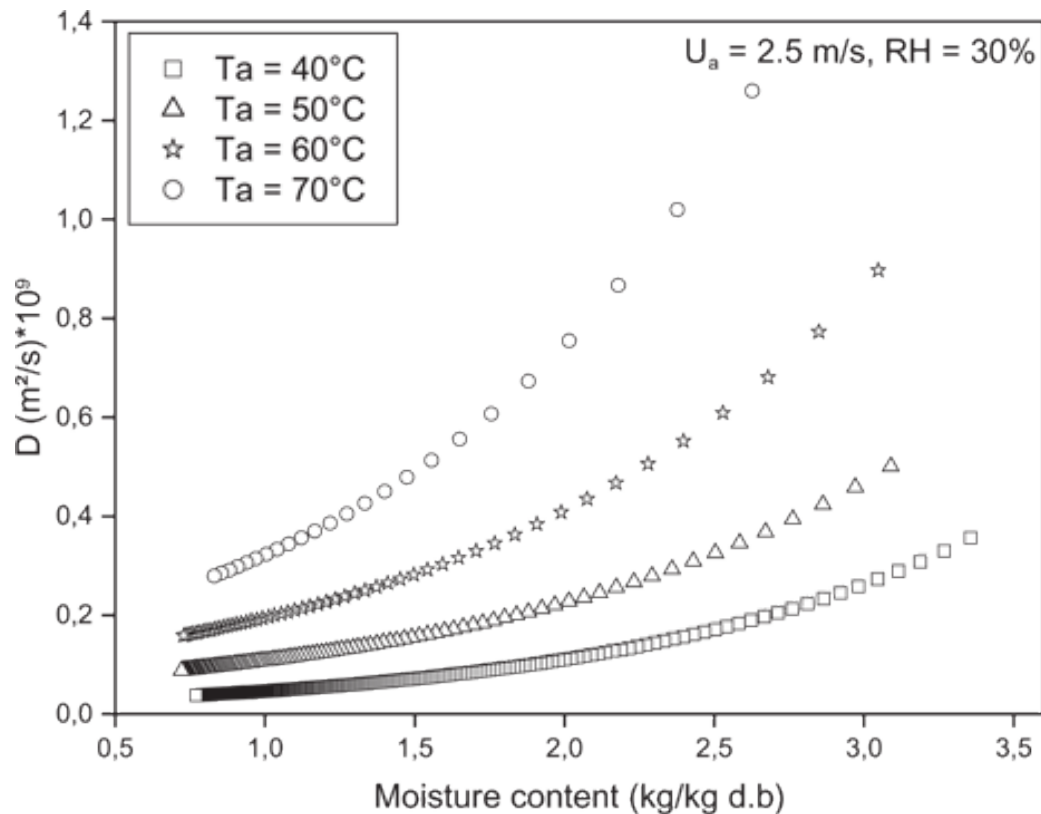


Figure 6: Drying rate of Sultana grape versus moisture content at different air temperatures.



### 3.4 Identification of the moisture diffusion

Figure 7 presents the evolution of the moisture diffusivity as function as moisture content of the sultana grape. at different temperatures and an air velocity equal to 1.5 m/s. these curves shown a significant increasing of the moisture diffusivity with the air drying temperature and a moderate increasing with the moisture content. Similar results have been reported by Kiranoudis et al. [29], Garau et al. [30], and Guiné et al. [31].



**Figure 7:** Moisture diffusivity of the grape estimated by numerical method at various temperatures.

The reduction of the moisture diffusivity with the reduction of the moisture content is generally considered as a normal behavior in biological products [22, 32, 33].

The variation of  $(D_{x1})$  versus  $(1/T)$  for Sultana grape is shown in Figure 7. By the analysis of the experimental data, it was revealed the existence of exponential relationship between these parameters.

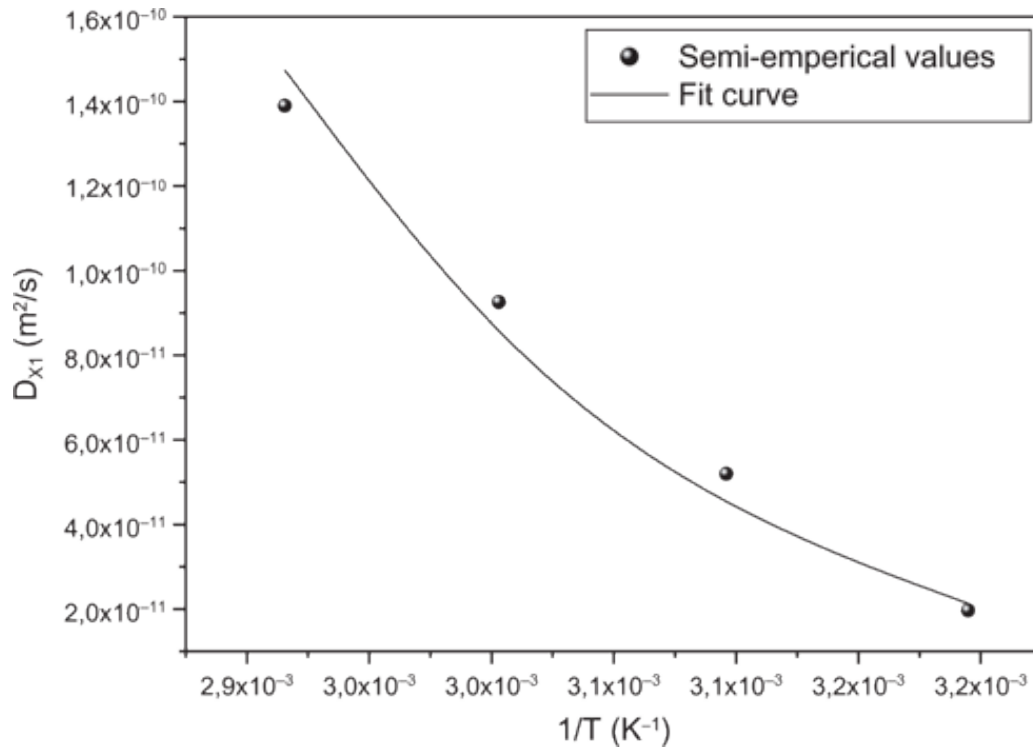


**Figure 8:** Variation of predicted diffusivity coefficient with  $(1/T)$  for seedless grape.

The variation of  $(D_{X2})$  with temperature for sultana grape was shown in Figure 9. We revealed a linear relationship between these parameters. Correlation coefficient ( $r$ ) of the fitted lines with experimental data was obtained as 0.9972.

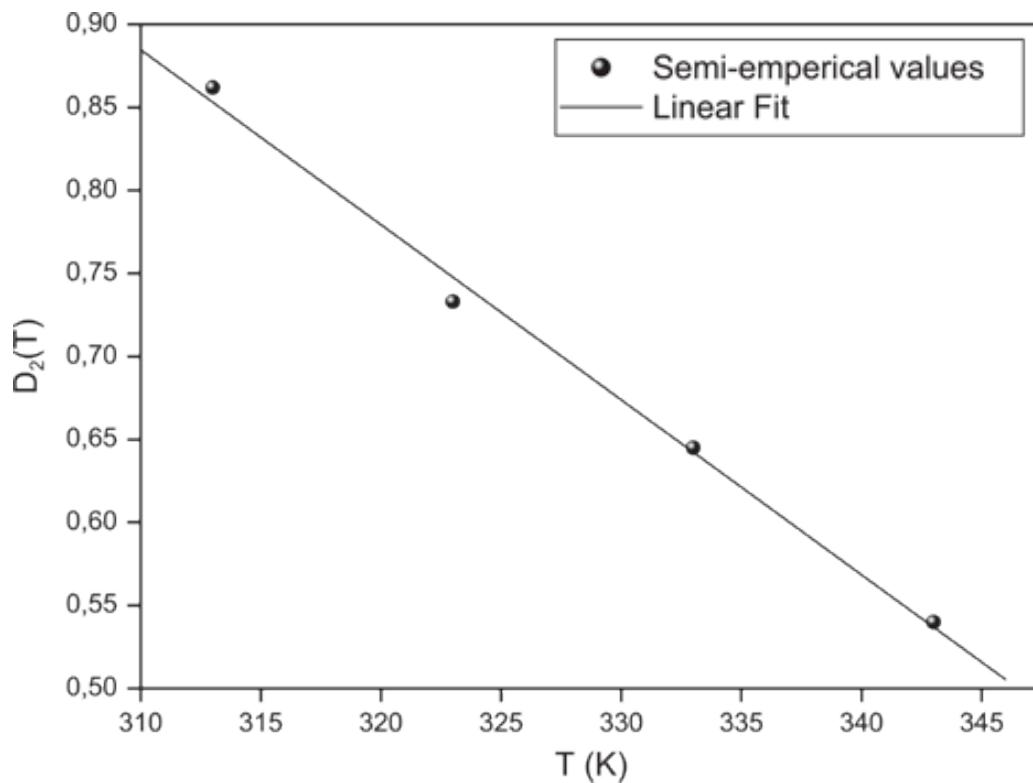


**Figure 9:** Variation of  $(D_{X2})$  with temperature for seedless grape.

Hence, taking into account relations from previous curves (Figure 8 and Figure 9) over the range of water content from 3.8 to 0.3 (kg /kg dry matter) and temperature values ranging from 40 up to 70 °C, our findings are quite similar to those reported by Doymaz [23], who found that the water diffusivity of grape varies between

$3.5610^{-10}$  ( $\text{m}^2/\text{s}$ ) and  $12.610^{-10}$  ( $\text{m}^2/\text{s}$ ). The water diffusivity of Sultana grapes is expressed by the following equation:

$$D(X, T) = 8.48 \times 10^{-2} \exp\left(-\frac{57.56}{RT}\right) \exp((0.01T - 4.149)X) \quad (27)$$

In order to compare our semi-empirical diffusivity correlation with those reported in literature, the moisture diffusivity versus moisture content obtained with eq. 27 and with two others correlations selected from Saravacos [34] and Raghavan et al. [35] for seedless grapes were compared (Table 3). It can be noted that our results is very close to that found in literature for the cited references. The slight difference between the compared data can be explained mainly by the estimating methods of moisture diffusivity, what stresses the need for standardization and benchmarking of moisture diffusivity measurements. Otherwise, it should be noted that our activation energy value (57.56 kJ/mol) is far from to that found by Azzouz et al. [8], using a numerical approach to estimate the moisture diffusivity of grape and identifies a value of activation energy equal to 34,87 kJ/mol. This difference can be attributed mainly to the grapes varieties and the measurements errors.

**Table 3:** Comparison of the estimated moisture diffusivity values with those reported in literature.

	X (kg/kg d.b)	T (°C)	D ( $\text{m}^2/\text{s}$ )
Present work	$0.72 \leq X \leq 3.08$	50	$8.810^{-11} \leq D \leq 5.10^{-10}$
	$0.72 \leq X \leq 3.05$	60	$1.610^{-10} \leq D \leq 8.8 \cdot 10^{-10}$
Raghavan et al. (1995)	$0.17 < X < 3.5$	50	$1.10^{-11} \leq D \leq 4.10^{-10}$
Saravacos (1986)	$0.15 \leq X \leq 2.4$	60	$5.10^{-11} \leq D \leq 2.5 \cdot 10^{-10}$

## 4 Conclusion

The equilibrium moisture content of seedless grape was determined at several temperatures 40, 50, 60 and 70 °C over the water activity range of 0.02–0.9, using the static gravimetric method. The desorption isotherms were found to decreases with increasing temperature at constant water activity. However, at constant temperature they increase with increasing water activity.

The shrinkage of seedless grape was determined, it presented a linear function of moisture content and an empirical equation of shrinkage was developed. This shrinkage was included into the numerical diffusion model.

The drying kinetics of seedless grape were established, their contained only falling periods. The drying rate increased when increasing the air temperature.

The moisture diffusivity of seedless grape was determined from convective drying kinetics by using numerical approach, these values were correlated to temperature and moisture content by an Arrhenius-type correlation. The coefficients of the obtained correlation were also correlated with the state variables (T and X) of the product using an exponential and linear functions. Moisture diffusivity increased with air temperature. According to our study, the shrinkage effect must not be neglected in moisture diffusivity for highly shrinking materials.

## Acknowledgement

We gratefully acknowledge Mr. Abderrazek ZAARAOUI, technician at the Heat and mass transfer laboratory (LETTM) of University of Tunis El Manar, Tunisia, for his help in carrying out the experiments.

## Nomenclature

$a_w$ : The water activity

C and K: The characteristic constant of the GAB model

$c_l$ : The concentration of the liquid phase ( $\text{kg}/\text{m}^3$ )

$c_s$ : The concentration of the solid phase ( $\text{kg}/\text{m}^3$ )

$D$ : The moisture diffusivity ( $\text{m}^2/\text{s}$ )  
 $D_0$ : The Arrhenius factor ( $\text{m}^2/\text{s}$ )  
 $E_a$ : The activation energy ( $\text{kJ/mol}$ )  
 $M_d$ : The dry mass ( $\text{kg}$ )  
 $M_f$ : The final mass ( $\text{kg}$ )  
 $M_v$ : The Vapor molar mass ( $\text{kg/mol}$ )  
 $n_{\text{exp-data}}$ : The number of experimental points  
 $n_{\text{param}}$ : The parameters number of the model  
 $P_{\text{v.sat}}$ : The saturation vapor pressure ( $\text{Pa}$ )  
 $r$ : The radial distance ( $\text{m}$ )  
 $\text{RH}$ : The relative humidity (%)  
 $U$ : The mass averaged velocity  
 $u_s$  and  $u_l$ : Velocities of solid and liquid phases ( $\text{m/s}$ )  
 $X_{\text{eqi}}$ : The experimental equilibrium moisture content  
 $X_{\text{eqcal}}$ : The calculated equilibrium moisture content  
 $X_m$ : The moisture content ( $\text{kg/kg dry matter}$ )  
 $\beta$ : The experimental shrinkage coefficient  
 $\rho$ : The total mass density ( $\text{kg/m}^3$ )  
 $\rho_s$ : The density of dry solid ( $\text{kg/m}^3$ )

## References

1. Touil A, Chemkhi S, Zagrouba F. Moisture diffusivity and shrinkage of fruit and cladode of opuntia ficus-indica during infrared drying. *J Food Process*. 2014;2014:1–9.
2. Mujumdar AS, Devahastin S. Fundamental principles of drying. In: Devahastin S, editors. *Guide to industrial drying*. Montreal, Canada: Exergex corp; 2000:1–22.
3. Janjai S, Mahayothee B, Lamler N, Bala BK, Precoppe M, Nagle M, et al. Diffusivity, shrinkage and simulated drying of litchi fruit (*Litchi chinensis* sonn). *J Food Eng*. 2010;96:214–221.
4. Mayor L, Sereno AM. Modelling shrinkage during convective drying of food materials. *J Food Eng*. 2004;61(3):373–386.
5. Giovanelli G, Zanoni B, Lavelli V, Nani R. Water sorption drying and antioxidant properties of dried tomato products. *J Food Eng*. 2002;52:135–141.
6. Azzouz S, Guizani A, Jomaa W, Belghith A. Moisture diffusivity and drying kinetic equation of convective drying of grapes. *J Food Eng*. 2002;55:323–330.
7. Hassini L, Azzouz S, Pecalski R, Belghith A. Estimate of potato convective moisture diffusivity from drying kinetics with correction for shrinkage. *J Food Eng*. 2007;39:47–56.
8. Azzouz S, Hermassi I, Toujani M, Belghith A. Effect of drying temperature on the rheological characteristics of dried seedless grapes. *Food Bioprod Process*. 2016;100:246–254.
9. Zogzas NP, Maroulis ZB, Marinou-Kouris D. Moisture diffusivity data compilation in foodstuffs. *Drying Technol*. 1996;14(10):2225–2253.
10. Nilnoni W, Thepa S, Janjai S, Bala BK. Finite element simulation for coffee (*Coffea arabica*). *Food Bioprod Process*. 2012;90:341–350.
11. AOAC. Official methods of analysis Vol. 15. Washington: Association of official chemists; 1990:934–936.
12. Spiess WE, Wolf WF. The results of the COST 90 project on water activity. *Phys Prop Foods*. 1983;83:65–91.
13. Labuza TP. Practical aspects of isotherm measurement and use. St. Paul, MN: American Association of Cereal Chemists; 1984.
14. Ouertani S, Azzouz S, Hassini L, Koubaa A, Belghith A. Moisture sorption isotherms and thermodynamic properties of Jack pine and palm wood: comparative study. *Ind Crops Prod*. 2014;56:200–210.
15. Djendoubi N, Boudhrioua N, Bonazzi C, Kechaou N. Drying of sardine muscles: experimental and mathematical investigations. *Food Bioprod Process*. 2009;87:115–123.
16. Madiouli J, Sghaier J, Lecomte D, Sammouda H. Determination of porosity change from shrinkage curves during drying of food material. *Food Bioprod Process*. 2012;90(1):43–51.
17. Bird RB, Stewart WE, Lightfoot EL. *Transport phenomena*. New York, NY: John Wiley and Sons, Inc.; 1960.
18. Ketelaars AA, Kaasschieter EF, Coumans WJ, Kerhaff PJ. The influence of shrinkage on drying behavior of clays. *Drying Technol*. 1994;12(7):1561–1574.
19. Incropera FD, Dewitt DP. *Fundamentals of heat and mass transfer*, 4th ed. New York: John Wiley and Sons, Inc.; 1996.
20. Patankar SV. *Numerical heat transfer and fluid flow*. New York: Hemisphere publishing Co.; 1980.
21. Erenturk S, Sahin Gulaboglu M, Gultekin S. Experimental determination of effective moisture diffusivities of whole and cut-rosehips in convective drying. *Food Bioprod Process*. 2010;88:99–104.

22. Saravacos GD, Maroulis ZB, Dekker M. Properties transport of foods. *Drying Technol.* 2001;19(9):2383–2384.
23. Doymaz I. Air-drying characteristics of tomatoes. *J Food Eng.* 2007;78:1291–1297.
24. Tripathy PP, Kumar S. Methodology for determination of temperature depend farmhouse transfer. Coefficients from drying kinetics: application to solar drying. *J Food Eng.* 2009;90(2):212–218.
25. Brunauer S, Emmett PH, Teller E. Adsorption of gases in multimolecular layers. *J Amercian Chem Soc.* 1938;60:309–319.
26. Wolf W, Spiess WE, Jung G. Sorption isotherms and water activity of food materials. New York: Elsevier Science Ltd; 1985.
27. Moriera R, Chenlo F, Vazquez MJ, Camean P. Sorption isotherms of turnip top leaves and stems in the temperature range from 298 to 328 K. *J Food Eng.* 2005;71:193–199.
28. Toujani M, Hassini L, Azzouz S, Belghith A. Drying characteristics and sorption isotherms of silverside fish (*Atherina*). *Int J Food Sci Technol.* 2011;46:594–600.
29. Kiranoudis C. T., Maroulis Z. B., Marinos-Kouris D., Saravacos G. D.. Estimation of the Effective Moisture Diffusivity from Drying Data. Application to Some Vegetables. *Developments in Food Engineering*; 1994:340–342. . DOI:10.1007/978-1-4615-2674-2\_106.
30. Garau MC, Simal S, Fermentia A, Rossello C. Drying of orange skin: drying kinetics modeling and functional properties. *J Food Eng.* 2006;75:288–295.
31. Guiné RP, Rodrigues AE, Figueiredo MM. Modeling and simulation of pear drying. *J Food Eng.* 2007;192:69–77.
32. Keey RB. Drying principles and practices. Oxford, NY: Pergamon Press; 1972.
33. Cherife. J. Fundamentals of the drying mechanism during air dehydration of foods. In: Mujumdar AS, editors. *Advances in drying Vol. 2.* New York: Hemisphere Publishing Corp; 1983:73–102.
34. Saravacos GD. Mass transfer properties of foods. In: Rao MA, Rizvi SSH, editors. *Engineering properties of foods.* New York: Marcel Dekker; 1986.
35. Raghavan GS, Tulasidas TN, Sablani SS, Ramaswamy HS. A method of determination of concentration dependent effective moisture diffusivity. *Drying Technol.* 1995;13(5–7):1477–1488.